

Article

Predictive Control Method of Reaming up in the Raise Boring Process Using Kernel Based Extreme Learning Machine

Guoye Jing^{1,2}, Wei Yan³ and Fuwen Hu^{3,*} 

¹ School of Civil and Resources Engineering, University of Science and Technology Beijing, Beijing 100083, China

² Mine Construction Branch, China Coal Research Institute, Beijing 100013, China

³ School of Mechanical and Material Engineering, North China University of Technology, Beijing 100144, China

* Correspondence: hfw@ncut.edu.cn

Abstract: Raise boring is an important method to construct the underground shafts of mines and other underground infrastructures, by drilling down the pilot hole and then reaming up to the desired diameter. Seriously different from the drilling operations of the mechanical parts in mechanized mass production, it is very difficult to obtain a good consistency in the construction environments of each raise or shaft, to be more exact, every construction process is highly customized. The underground bottom-up reaming process is impossible to be observed directly, and the rock breaking effect is very difficult to be measured in real-time, due to the rock debris freely falling under the excavated shaft. The optimal configurations of the operational parameters in the drilling and working pressures, torque, rotation speed and penetration speed, mainly depend on the accumulation of construction experience or empirical models. To this end, we presented a machine learning method, based on the extreme learning machine, to determine in real-time, the relationships between the working performance and the operational parameters, and the physical-mechanical properties of excavated geologic zones, aiming at a higher production or excavation rate, safer operation and minimum ground disturbance. This research brings out new possibilities to revolutionize the process planning paradigm of the raise boring method that traditionally depends on experience or subject matter expertise.

Keywords: underground construction; raise boring method; extreme learning machine; predictive control



Citation: Jing, G.; Yan, W.; Hu, F. Predictive Control Method of Reaming up in the Raise Boring Process Using Kernel Based Extreme Learning Machine. *Processes* **2023**, *11*, 277. <https://doi.org/10.3390/pr11010277>

Academic Editors: Jie Zhang and Wei Sun

Received: 2 December 2022

Revised: 3 January 2023

Accepted: 10 January 2023

Published: 14 January 2023



Copyright: © 2023 by the authors. Licensee MDPI, Basel, Switzerland. This article is an open access article distributed under the terms and conditions of the Creative Commons Attribution (CC BY) license (<https://creativecommons.org/licenses/by/4.0/>).

1. Introduction

As the “throat” channel into the underground spaces, boreholes or shafts play important roles, such as ventilation, transportation and safety. The traditional borehole construction method, based on drilling and blasting, has a low level of mechanization and involves a harsh operating environment for the personnel in the borehole, where serious occupational injuries and safety accidents can occur. In particular, it is difficult to achieve continuous, automated and intelligent operations, when using the blasting method. In this regard, the raise boring construction method has become the main underground construction method, which is widely used in the underground mineral extraction, hydroelectric power generation, pumped storage power stations, railroad and highway tunnels, underground oil storage, gas storage, nuclear waste storage and carbon dioxide sequestration.

The raise boring method is a construction process used to excavate shafts by bottom-up reaming the pilot hole using drill rigs [1], which mainly includes two operational processes (see Figure 1). The first operation is to use the drill bit to top-down drill a small diameter hole (pilot hole, see Figure 1a) as a guide to the reaming up operation. In the process of drilling down the pilot hole, the drill pipe is gradually increased by the established design, until the bit is connected with the lower horizontal roadway. In this process, the rock debris is carried out of the shaft bore by the circulating wash media, and the drill bit is

removed, then it switches to the bottom-up reaming process, selecting the type of reaming bit and drilling parameters, according to the formation rock conditions, and reaming from the bottom to the top until the reaming drill penetrates from the upper space (ground or tunnel) (see Figure 1b). During back reaming, the rock debris falls down to the lower horizontal roadway because of gravity and it is then transported out by the loaders or other loading equipment.

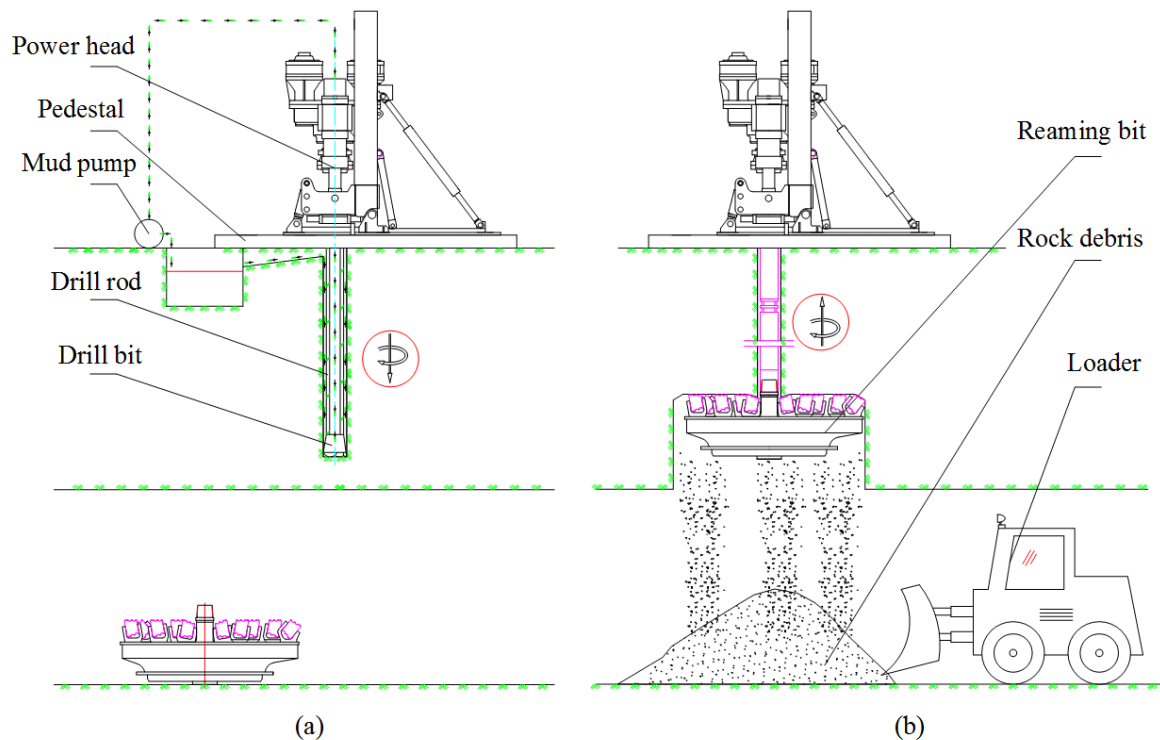


Figure 1. Diagram of the raise boring method: (a) pilot hole drilling (top-down); (b) back reaming (bottom-up).

Owing to the complex rock stratum, it is very difficult to reach a good consistency in the construction environments of each raise or shaft, thereby each construction process is highly customized. During the raise boring machine (RBM) operation, the operator cannot directly observe the underground bottom-up reaming process, and it is difficult to measure the rock breaking effect by the sensors, in real-time. In addition, during the reaming process, the drilling tool system is subjected to great external forces, which can easily lead to safety accidents. For this reason, Jing et al. (2020) [2] studied the failure of the RBM load-bearing threaded joints, using a failure analysis, and thus improved the parts. Jing et al. (2021) [3] analyzed the load of the drill pipe joints and improved the load distribution by improving the incomplete threads, thus preventing the occurrence of drill pipe fracture accidents.

These uncertainties and the invisibility seriously prevent the RBM from selecting the best engineering performance and operating parameters, thus reducing the production or excavation rate. Therefore, Hu et al. (2021) [4] determined the optimal values of the pulling force of the reaming, working torque, rotational speed of drilling and penetration speed of the RBM under different parameters, through experiments and data analyses, and studied their relationship in the process of rock breaking, so as to improve the rock breaking efficiency of the RBM. Hu et al. (2022) [5] developed a digital twin-driven decision making prototype system for the RBM process, which provided a great convenience for the complex RBM process planning.

The core of the RBM process planning is to determine the relationships between the drilling rig performance, the operating parameters and the physical and mechanical prop-

erties of the excavated geological zone. However, the current process planning method is mostly experience-dependent, which causes the low generalization performance and lacks the dynamic adaptability to the uncertainties. For instance, the research in [6] presented an empirical model, based on the indentation index and the rock cutting test, to estimate the performance of the RBM and the parameters, such as the thrust and torque of the RBM. Shaterpour-Mamaghani et al. (2018) [7] studied the effects of the physical and mechanical properties and the rock properties, on the performance of the drilling rigs by simple and multiple regression methods, and established an empirical model, to estimate the performance and operating parameters of the ream drilling tools. Further, they proposed an empirical model for predicting the vertical and inclined RBM guide hole and the reaming hole, by using the rock properties and guide hole drilling process parameters [8]. The experimental results show that the lifting slope and the prediction of the guide hole drilling parameters are the most important for the efficiency of the RBM. Shaterpour-Mamaghani et al. (2022) [9] considered two different deterministic methods (direct and indirect) to predict the relevant parameters of the RBM, through full-scale linear cutting tests and the rock physical and mechanical properties.

The RBM exerts the driving force and the working torque on the drill pipe during the reaming process, and the drill bit rotation is the basic motion used to break the rock. For the small RBM, due to the small diameter and depth of the borehole, the RBM is generally controlled by a single hydraulic motor drive, which is meshed with large and small gears, to decelerate in order to achieve the required technical parameters for drilling. For the large RBM, the torque required for the reaming is greater, the speed is slower, and the drilling speed cannot be too fast, otherwise it will affect the drilling efficiency of the guide hole. Therefore, a large RBM generally uses a multi-hydraulic motor drive control system to decelerate through pinion-driven large gear meshing, to meet the process requirements of the RBM. As stated previously, most of the current predictive control models are empirical and generally based on the relationship between the construction site and the physical and mechanical properties of the rock, and it requires an extremely high reliability of the data, so there are still many problems, based on this relatively traditional predictive control model.

The model predictive control (MPC) [10–12] is a control method, based on the predictive models, the rolling optimization and the feedback correction, which uses models to predict the future information of the system for the optimal control and is adopted in a large number of industrial practices [13,14], such as in aerospace [15], wind farms [16], biology [17], rock [18], production [19], etc. However, most industrial objects are nonlinear, and the effectiveness and robustness of many predictive control methods for the real-time optimization are deficient, making many successful linear system models poorly exploited. A large number of MPCs, based on neural networks, were subsequently investigated, such as the ant colony optimization (ACO) [20], gradient descent (GD) [21], genetic algorithm (GA) [22], support vector machine (SVM) [23], back propagation (BP) [24] and radial basis function (RBF) [25]. However, the learning efficiency and the generalization ability of these predictive control algorithms were far below the industrial requirements. To address this bottleneck, Yang et al. (2015) [26] proposed an autonomous mobile robot path-tracking predictive control algorithm, based on an extreme learning machine (ELM), to achieve a higher accuracy and performance. Wong et al. (2016) [27] established an online sequential extreme learning machine (OSELM) predictive control model, based on the ELM to replace the traditional PID controller. Yan et al. (2013) [28] proposed a minimal-extreme predictive control method to solve uncertain nonlinear systems.

In the raise boring process, the realization of the real-time predictive control of the drilling parameters is of great significance, in order to guide the parameter setting of the drilling rig in the actual drilling process, to make production plans, to complete the engineering handover and to improve the production efficiency of the drilling rig. However, various drilling parameters influence each other and there is a complex nonlinear relationship. To address the problems of the low generalization performance and the lack of dynamic adaptability regarding the uncertainties in the RBM during the ream drilling,

such as the rock deformation, instability and even collapse caused by some uncertainties, an intelligent predictive control method, based on the ELM is proposed in this paper, to determine the relationship between the work performance of the excavated geological zone and the operational parameters, and the physical and mechanical properties, in real time.

Among the current big data analysis and machine learning methods, the ELM is widely adopted in the predictive control models, because it has a faster training speed, a good generalization performance and a higher learning accuracy than the traditional machine learning methods [29,30]. It can be applied well to the predictive control of the parameters related to ream drilling. It has a good application effect in the process of the practical application, such as the parameter regression analysis and prediction, and the fault diagnosis and classification. The ELM is employed to train the drilling parameter data in the process of ream drilling, to obtain the predictive control of the penetration speed. It can estimate the construction period and facilitate the construction handover and arrangement. Djerioui et al. (2019) [31] compared the support vector machine with the ELM in water quality monitoring, and concluded that the ELM has a better learning time and a faster training speed than the SVM. Gao et al. (2022) [32] designed a monitoring condition and a predictive life control model, based on the ELM and transfer learning for the turning tool wear. MontazeriGh et al. (2022) [33] proposed a fault diagnosis system, based on the OSELM to update and monitor any number of new training samples. Cao et al. (2012) [34] established an improved voting classification, based on the voting-based extreme learning machine (VELM).

In this work, the drilling rig-related data of the drilling process are trained by the ELM and the kernel-based extreme learning machine (KELM), to obtain the predictive control of the pulling force of the reaming, the working torque, the rotational speed of the drilling, the penetration speed, and the working bit condition classification in the drilling process. In the process of the predictive control of the ream drilling parameters of the RBM, the mean square error MSE and the determination coefficient R^2 of the model are derived, by comparing the output true values with the predicted values of the ELM model, and then the MSE and R^2 are used to correct the predicted values of the model, to obtain more accurate prediction values, and finally, the optimized prediction model is controlled and the output for the intelligent monitoring of the RBM is obtained. For clarity, we explain the machine learning-based predictive control approach of the raise boring process in the Figure 2.

The remainder of the article is structured as follows. Section 2 briefly reviews the basic concept and background knowledge of the ELM and KELM. Section 3 describes the experimental study and presents the ELM-based predictive control model for the drilling parameters of the RBM reaming and the intelligent monitoring model for the drilling status of the RBM, based on the ELM and KELM. Section 4 provides a comparative discussion of the experimental results. This article concludes with Section 5. Table 1 lists the nomenclature of the terms in this article, and Table 2 lists the abbreviations of the terms used in this article.

Table 1. Nomenclature of the terminologies.

No.	Terms	Symbols
1	Working pressure	N
2	Pulling force of reaming	F
3	Working torque	T_q
4	Weight of reaming bit	W_{bit}
5	Penetration speed	v
6	Desired output	Y
7	Pilot hole diameter	d
8	Input weight	W_i

Table 1. Cont.

No.	Terms	Symbols
9	Output layer neuron	Y_i
10	Training error	ξ_i
11	Identity matrix	I
12	Work ratio of rock breaking	a_z
13	Rotation speed of drilling	n
14	Weight of drilling rods	W_{rods}
15	Reaming diameter	D
16	Rock compressive strength	σ_c
17	Input layer neuron	X_i
18	Offset of hidden layer unit	b_i
19	Determination coefficient	R^2
20	Kernel function matrix	Ω_{ELM}
21	Output weight	β_i

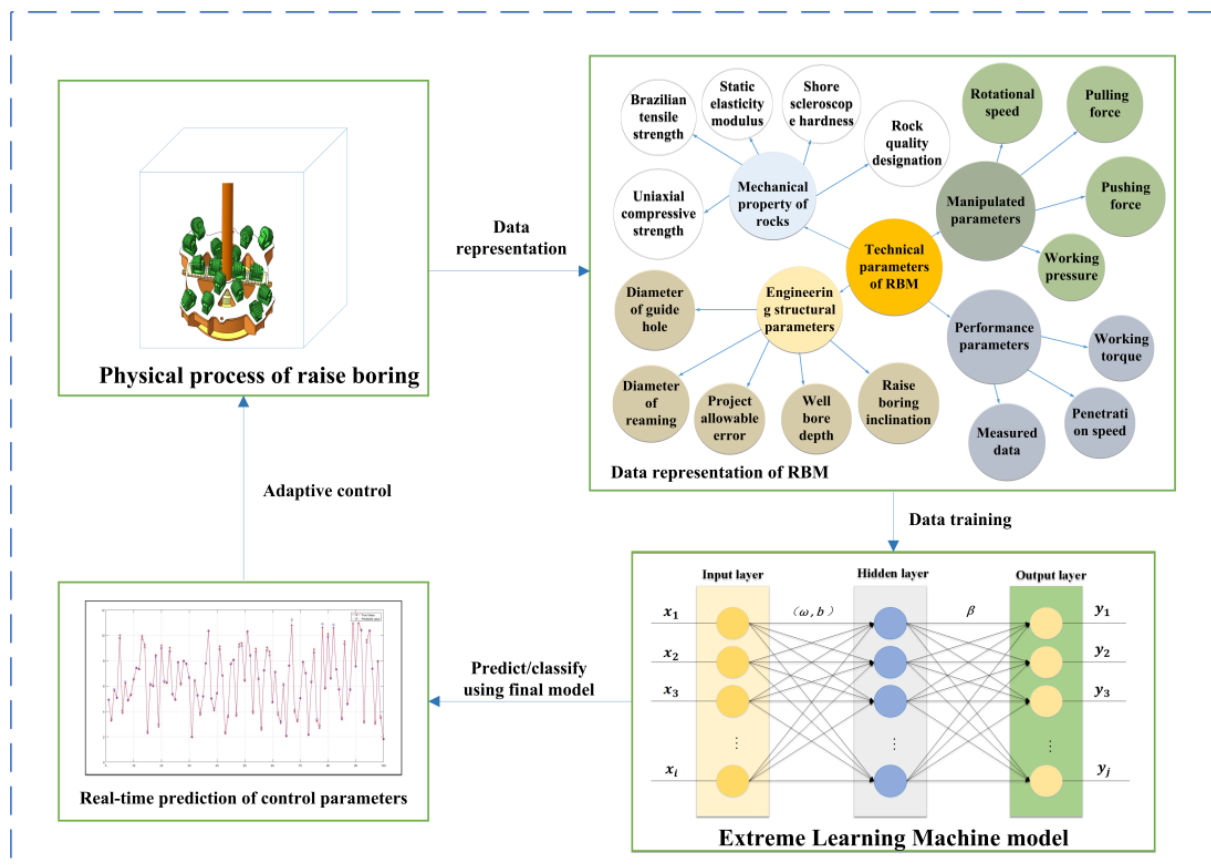


Figure 2. Predictive control framework of the raise boring process using the machine learning method.

Table 2. Abbreviations of the terminologies.

No.	Terms	Symbols
1	Extreme Learning Machine	ELM
2	Kernel Based Extreme Learning Machine	KELM
3	Multi-Kernel Extreme Learning Machine	MKELM
4	Voting Based Extreme Learning Machine	VELM
5	Model Predictive Control	MPC
6	Gradient Descent	GD

Table 2. Cont.

No.	Terms	Symbols
7	Radial Basis Function	RBF
8	Support Vector Machine	SVM
9	Ant Colony Optimization	ACO
10	Genetic Algorithm	GA
11	Back Propagation	BP
12	Single-Hidden Layer Feedforward Neural Network	SLFN
13	Particle Swarm Optimisation	PSO
14	Back Propagation Neural Network	BPNN
15	Online Sequential Extreme Learning Machine	OSELM
16	Shore Scleroscope Hardness	SSH
17	Rock Quality Designation	RQD
18	Mean Square Error	MSE
19	Raise Boring Machine	RBM

2. Methods

2.1. Extreme Learning Machine

The ELM is a machine learning method, based on the single hidden layer feedforward neural network (SLFN) proposed by Professor Huang Guangbin of Nanyang University of Technology, in 2004 [35]. It is suitable for supervised learning and unsupervised learning problems [36–39], compared with the back propagation neural network (BPNN) [40,41]. The ELM algorithm model can randomly set the connection weight between the input layer and the hidden layer and the threshold of the hidden layer, and there is no need to adjust it after setting. At the same time, in the network structure of the ELM, the connection weight value β between the hidden layer and the output layer can be determined by the generalized inverse matrix theory. Finally, through the test data and the connection weight value β obtained, the network output can be calculated to complete the prediction of the data.

In the Figure 3, where W is the input weight, b is the deviation matrix. $H(x)$ is the output of the hidden layer node, β is the connection weight between the hidden layer and the output layer.

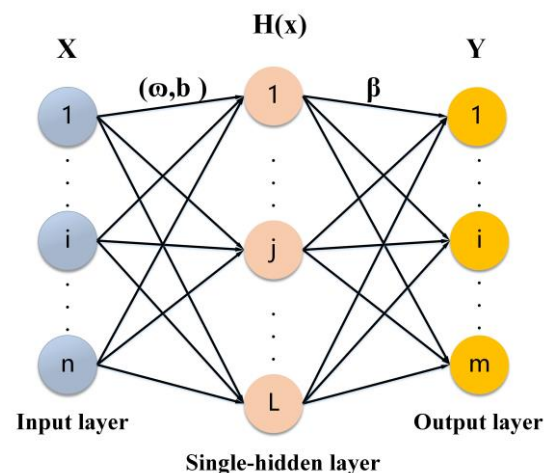


Figure 3. ELM network structure chart.

For single hidden layer neural networks with N samples. $X_i = [x_{i1}, x_{i2}, \dots, x_{in}]^T$ is the input layer neuron, it is the n -dimensional data. $Y_i = [y_{i1}, y_{i2}, \dots, y_{im}]^T$ is the output layer neuron, it is the m -dimensional data. $H(x) = [h_1(x), h_2(x), \dots, h_L(x)]$ is the output matrix of the neurons in the hidden layer, it is the number of L hidden layer nodes. $h_i(x)$ is the output of the first hidden layer node. The n -dimensional data of the input layer and the

m-dimensional data of the output layer are determined by the actual training model, When the ELM neural network has L hidden layer nodes, it can be expressed as:

$$\sum_{i=1}^L \beta_i g(W_i \cdot X_j + b_i) = p_j, j = 1, 2, \dots, N \quad (1)$$

where β_i is the output weight, $W_i = [w_{i,1}, w_{i,2}, \dots, w_{i,n}]^T$ is the input weight, b_i is the offset of the i hidden layer unit. $W_i \cdot X_j$ represents the inner product of W_i and X_j . g is the activation function. The commonly used activation functions are the sinusoidal function, tangent function and Sigmoid function. Their expressions are as follows:

$$g(x) = \sin(x) = \frac{e^{ix} - e^{-ix}}{2i} \quad (2)$$

$$g(x) = \tan(x) = \frac{e^{ix} - e^{-ix}}{i(e^{ix} + e^{-ix})} \quad (3)$$

$$g(x) = \frac{1}{1 + e^{-x}} \quad (4)$$

For the neural networks, the goal of training and learning is to minimize the error between the output value and the actual value, that is, the norm of the difference between the output value and the actual value is 0. It can be expressed as:

$$\sum_{j=1}^N \| p_j - y_j \| = 0 \quad (5)$$

According to Formula (1), the goal of the neural network is to find out β_i , W_i and b_i , which satisfy Formula (6):

$$\sum_{i=1}^L \beta_i g(W_i \cdot X_j + b_i) = y_j, j = 1, 2, \dots, N \quad (6)$$

Assume $g(W_i \cdot X_j + b_i) = H(x) = H$, Then $H\beta = Y$. Where H is the output of the hidden layer node, β is the output weight, and Y is the desired output. It can be expressed as:

$$H(W_1, \dots, W_L, b_1, \dots, b_L, X_1, \dots, X_L) = \begin{bmatrix} g(W_1 \cdot X_1 + b_1) \dots g(W_L \cdot X_1 + b_L) \\ \vdots \\ g(W_1 \cdot X_N + b_1) \dots g(W_L \cdot X_N + b_L) \end{bmatrix}_{N \times L} \quad (7)$$

$$\beta = \begin{bmatrix} \beta_1^T \\ \vdots \\ \beta_L^T \end{bmatrix}_{L \times m} \quad Y = \begin{bmatrix} Y_1^T \\ \vdots \\ Y_N^T \end{bmatrix}_{N \times m}$$

The purpose of training the single hidden layer neural network is to obtain the expected weights \hat{W}_i of the input weights W_i , the expectation of the bias matrix \hat{b}_i and the expectation $\hat{\beta}_i$ of the output weight β . It can be expressed as:

$$\| H(\hat{W}_i, \hat{b}_i) \hat{\beta}_i - Y \| = \min_{W, b, \beta} \| H(\hat{W}_i, \hat{b}_i) \hat{\beta}_i - Y \| \quad (8)$$

Which $i = 1, \dots, L$, the above formula is also equivalent to minimizing the loss function, that is, taking the minimum value of E , that is:

$$E = \sum_{j=1}^N \left(\sum_{i=1}^L \beta_i g(W_i \cdot X_j + b_i) - y_j \right)^2 \quad (9)$$

When the ELM algorithm is adopted to solve the above problems, the algorithm model can randomly determine the input weight W_i and the bias values of the hidden layer b_i . In this way, the output matrix of the hidden layer H is uniquely determined. The problem of training the single hidden layer neural network can be transformed by solving a linear system $H\beta = Y$. The expected value $\hat{\beta}$ of the output weight β is:

$$\hat{\beta} = H^+Y \quad (10)$$

where H^+ is the generalized inverse matrix of H .

Then, the mean square error MSE and the determination coefficient R^2 are selected to judge the accuracy of the model learning effect. The mean square error is a measure that reflects the degree of difference in the estimator. It can be expressed as:

$$MSE(\hat{y}_i) = \frac{1}{N} \sum_{i=1}^N (\hat{y}_i - y_i)^2 \quad (11)$$

The determination coefficient R^2 also becomes the goodness-of-fit and is the square of the correlation coefficient. Its size determines the closeness of the correlation between the parameters. The closer the determination coefficient is to 1, the higher the independent variable explains the dependent variable, on the contrary, the closer it is to 0, the lower the reference value. It can be expressed as:

$$R^2 = \frac{\sum_{i=1}^N (\hat{y}_i - \bar{y})^2}{\sum_{i=1}^N (y_i - \bar{y})^2} \quad (12)$$

where N is the number of samples in Formulas (11) and (12), where y_i is the actual value of the variable, \bar{y} is the average value of the variable and \hat{y}_i is the estimated value of the variable. In this paper, these two evaluation parameters are used to evaluate the learning effect of the model. when the ratio of the mean square error to the corresponding parameters is less than 0.1, and the determination coefficient is greater than 0.9, it is considered that the learning effect of the model meets the requirements.

2.2. Kernel-Based Extreme Learning Machine

The ELM neural network model is prone to unstable training results and a poor generalization ability when it is used to classify and predict the drilling conditions. A drilling condition classification model, based on the KELM, is established in this paper. The KELM is an improved algorithm in which the kernel function idea of the SVR is introduced into the ELM by Huang of Nanyang University of Technology [42,43]. Compared with the ELM, this algorithm has a better prediction performance and a more stable performance. Kang et al. (2020) [44] established the health detection model of a concrete dam, based on the KELM, and obtained the effective safety monitoring data, which proves the prediction feasibility of the KELM. Fu et al. (2016) [45] studied the plate impact position prediction experiment, based on the KELM. Shamshirband et al. (2015) [46] used the KELM to predict the daily total solar radiation at maximum and minimum temperatures. Liu et al. (2021) [47] proposed a data classifier, based on the particle swarm optimization (PSO) and the kernel function extreme learning machine. Zhang et al. (2018) [48] studied a classification model of the EEG signals in moving images, based on the multi-kernel extreme learning machine (MKELM). Chen et al. (2016) [49] analyzed the prediction models of a Parkinson's diagnosis,

using the ELM and KELM, respectively. Compared with the ELM, the KELM has the advantage of introducing a regularization coefficient C for the output weight β on the basis of the ELM [43], used to weigh the training errors and the output weights. It can be expressed as:

$$\min \frac{1}{2} \|\beta\|^2 + \frac{1}{2} C \sum_{i=1}^n \|\zeta_i\|^2 \quad (13)$$

$$\text{s.t. } h(x_i)\beta = y_i^T - \zeta_i^T, \quad i = 1, 2, \dots, n$$

where ζ_i is the training error and $h(x_i)$ is the hidden layer feature mapping function. According to the KKT optimization condition [42], the solution is obtained:

$$\beta = H^T \left(HH^T + \frac{I}{C} \right)^{-1} Y \quad (14)$$

where I is the unit matrix, replacing the random matrix HH^T of the ELM neural network with the kernel function matrix Ω_{ELM} , to introduce the kernel function matrix [42], as follows:

$$\begin{cases} \Omega_{ELM} = HH^T \\ \Omega_{ELM_{i,j}} = h(x_i)h(x_j) = K(x_i, x_j) \end{cases} \quad (15)$$

where $K(x_i, x_j)$ is the element of row i and column j of the kernel function matrix Ω_{ELM} .

For the ELM, its objective function $F(x)$ can be expressed as a matrix:

$$F(x) = h(x) \times \beta = H \times \beta = Y \quad (16)$$

where x is the input vector, $h(x)$ and H are the hidden layer node output, β is the output weight, Y is the expected output. Then, the output function can be expressed as:

$$F(x) = \begin{bmatrix} K(x, x_1) \\ \vdots \\ K(x, x_m) \end{bmatrix}^T \left(\Omega_{ELM} + \frac{I}{C} \right)^{-1} Y \quad (17)$$

3. Experimental Study

When using the RBM for production, the operating parameters of the rig are the working pressure and the rotational speed of the drilling, and the performance parameters are the working torque and the penetration speed. Shaterpour-Mamaghani et al. (2018) [7] fit a large number of data about the actual construction of the drilling rig in different strata, and produced the model with the largest goodness-of-fit R^2 as the torque best linear fitting model, to determine the torque in the drilling process. The empirical model of the working torque T_q fitting can be expressed as follows:

$$T_q = 0.26 \times \sigma_c - 0.44 \times \text{SSH} + 52.50 \quad (18)$$

where σ_c is the uniaxial compressive strength in MPa, and SSH is the shore scleroscope hardness.

Through the linear regression analysis of the working torque and the working pressure, the pressure needed to break the rock is expressed as N and the pulling force required by the RBM is expressed as F . Then, they can be represented as:

$$F_{thrust} = 11.533 \times T_q + 356.2 \quad (19)$$

$$N = \frac{F_{thrust}}{k} - W_{bit} \cdot g - W_{rods} \cdot g \quad (20)$$

where W_{bit} is the weight of the reaming bit, and W_{rods} is the weight of the drilling rods.

According to the energy conservation formula proposed by Hu et al. (2022) [5], the penetration speed can be expressed as:

$$v = \frac{T_q \cdot 2\pi n}{\frac{1}{4}\pi(D^2 - d^2) \cdot a_z - N} \tag{21}$$

where v is the penetration speed, it depends on the rock’s mechanics, the hob tooth structure and the drilling pressure. n is the speed of the rotation. a_z is indicated by the ratio of the broken rock to broken rock. D represents the diameter of the reaming hole. d represents the diameter of the guide hole.

With the fitting of the drilling data, the relationship between the rotational speed of the drilling rig and the characteristic parameters of the rock in the process of reaming is obtained. It can be expressed as:

$$n = 0.01 \times RQD - 0.04 \times E_{sta} + 3.79 \tag{22}$$

$$a_z = (-0.01 \times \sigma_t - 0.0016 \times E_{sta} + 0.36)^{-1} \tag{23}$$

where RQD is the rock quality designation in %, E_{sta} is the static elasticity modulus in GPa. σ_t is the Brazilian tensile strength in MPa.

According to the formula, the correlation of the drilling rig working data under different working conditions is analyzed, and the result is shown in the Figure 4:

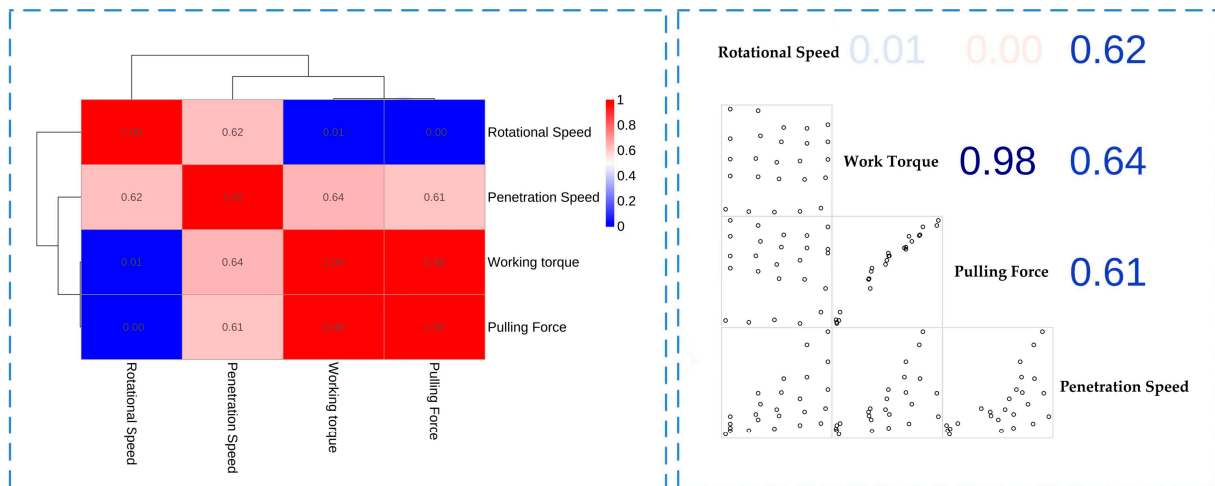


Figure 4. Correlation analysis diagram of the drilling parameters.

In the correlation matrix graph, the upper triangle of the matrix is the correlation coefficient among the parameters, and the lower triangle is the scatter distribution map of the data, and the correlation heat map is a conversion of the regularized matrix data into color tones, where each cell corresponds to an attribute of the ream drilling data. It can be seen from the figure that the parameter that has the greatest influence on the penetration speed is the working torque, which is positively correlated with the pulling force of the reaming, while the rotational speed has little effect on the pulling force of the reaming and working torque, and the correlation between the rotational speed of the drilling and the pulling force of the reaming is roughly the same. Through the above analysis and the experience of engineers, we can roughly derive the correlation of the working pressure, working torque, penetration speed and rotational speed, and determine the main technical parameters during the ream drilling process, which lays the foundation for the ELM predictive control experiments.

In the prediction experiment of the reaming data set by using the ELM, it is necessary to normalize the data first, and then divide the data into a training data set, a test data set and a construction experiment data set. The training data set is used to train the

model to obtain the prediction model, and the test data set is used to test the prediction model. If the prediction model does not meet the requirements, it is necessary to adjust the network structure of the ELM until it meets the requirements, in order To determine the final prediction model. Finally, the successful prediction model can be used to predict the relevant drilling parameters, monitor the drilling conditions and set the drilling parameters of the predicted completion through the operator console, on the basis of which the drilling control is carried out and it completes the rock-breaking tasks. Figure 5 is the flow chart of the intelligent predicting and monitoring for the ream drilling of the RBM.

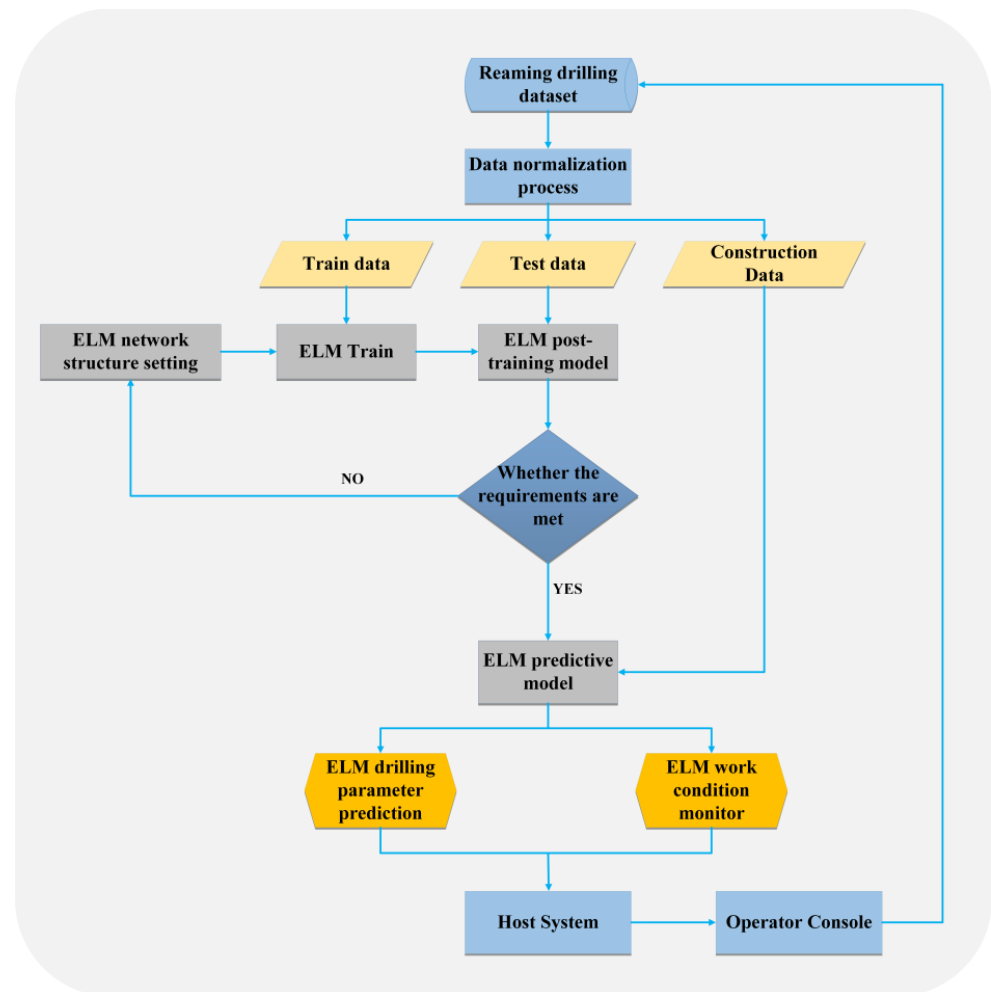


Figure 5. Flow chart of the intelligent predictive control for reaming up.

3.1. Data Processing of the Reaming

First of all, the data from the reaming need to be processed. From the point of view of the rig equipment, the main factors affecting the ream drilling are the working pressure, working torque, penetration speed and rotational speed of the drilling. According to the data measured by the experiment in this paper, the ELM algorithm experiment is carried out by selecting the working pressure, working torque, penetration speed and rotational speed. The experiment of the ELM algorithm needs a large data set as support. In this work, 2000 groups of sensor data are selected for the experiments.

3.2. Data Construction of the Training Set and the Test Set

Construction of the training set and the test set samples of the ELM algorithm. In order to make the prediction results of the ELM algorithm model more accurate, this research uses the randperm function to help build the training set and the test set of the algorithm

model. The purpose of this function is to randomly disrupt a sequence of numbers. Using this function, 1850 groups of drilling rigs are randomly selected as the training samples out of 2000 groups of drilling rigs running under different working conditions, and the remaining 150 groups are used as the test samples.

3.3. Data Normalization

The data of the reaming are normalized. When the ELM algorithm is adopted to predict the reaming parameters of the RBM, among the relevant parameters involved in the algorithm, are the unit of penetration speed (mm/min), the unit of the working pressure (kN), the unit of the working torque (kN·m), and the unit of the rotational speed of drilling (r/min). The units of each quantity are different, which will cause dimensional differences and adversely affect the prediction accuracy of the ELM algorithm model. To make the prediction results more accurate, this work uses the mapminmax function [50] to normalize each row of the data to be processed to $[-1, 1]$. In the input matrix, the minimum value of the row element is mapped to -1 , and the maximum value of the row element is mapped to 1 . The principle of the mapminmax function can be expressed by the following formula:

$$y = \frac{(y_{max} - y_{min}) \times (x - x_{min})}{x_{max} - x_{min}} + y_{min} \quad (24)$$

3.4. Prediction of the Reaming Parameters

3.4.1. Prediction of the Penetration Speed

The penetration speed of the reaming refers to the displacement of the bit per unit time, which is not only an important parameter to reflect the drilling efficiency, but also a symbol to measure the capacity of the drilling rig. Its speed will have a direct impact on the comprehensive economic benefits of the drilling project. Therefore, the prediction experiment of the penetration speed is carried out first, and after the data preparation is completed, Formula (18) is used to normalize it. To determine the relationship between the penetration speed and the working pressure, the working torque and the rotational speed of drilling, the output of the ELM algorithm model is set as the penetration speed sensor data, and the input is the working pressure, the working torque and the rotational speed of the drilling sensor data.

Firstly, the training function is constructed according to the algorithm principle of the ELM. In the training function, the training set data Pn_train is composed of the working pressure, working torque and rotational speed of the drilling, and the penetration speed training set data Tn_train are taken as the independent variables of the training function. In the independent variable of the ELM training function, we also need to set the corresponding number of hidden layer neurons, transfer function and training function category (regression: 0, classification: 1). The output of the training function is the input weight matrix IW , bias matrix B , hidden layer weight matrix LW , transfer function TF and training function category $TYPE$.

The output of the training function and the penetration speed test data set Pn_test are used as the input of the ELM prediction function. The output of this prediction function is the predicted penetration speed of the corresponding test set. The predicted penetration speed is only a dimensionless value of $[-1 \sim 1]$. It needs to be further de-normalized, so that the final predicted penetration speed can be obtained. Then we calculate the mean square error MSE and the determination coefficient R^2 between the real value and the predicted value of the test set, in which the mean square error can be calculated by using Formula (11) or the MSE function. When calculating the determination coefficient, Formula (12) is used to calculate the determination coefficient. The predicted value of the penetration speed is compared with the real value, and the result is shown in the Figure 6.

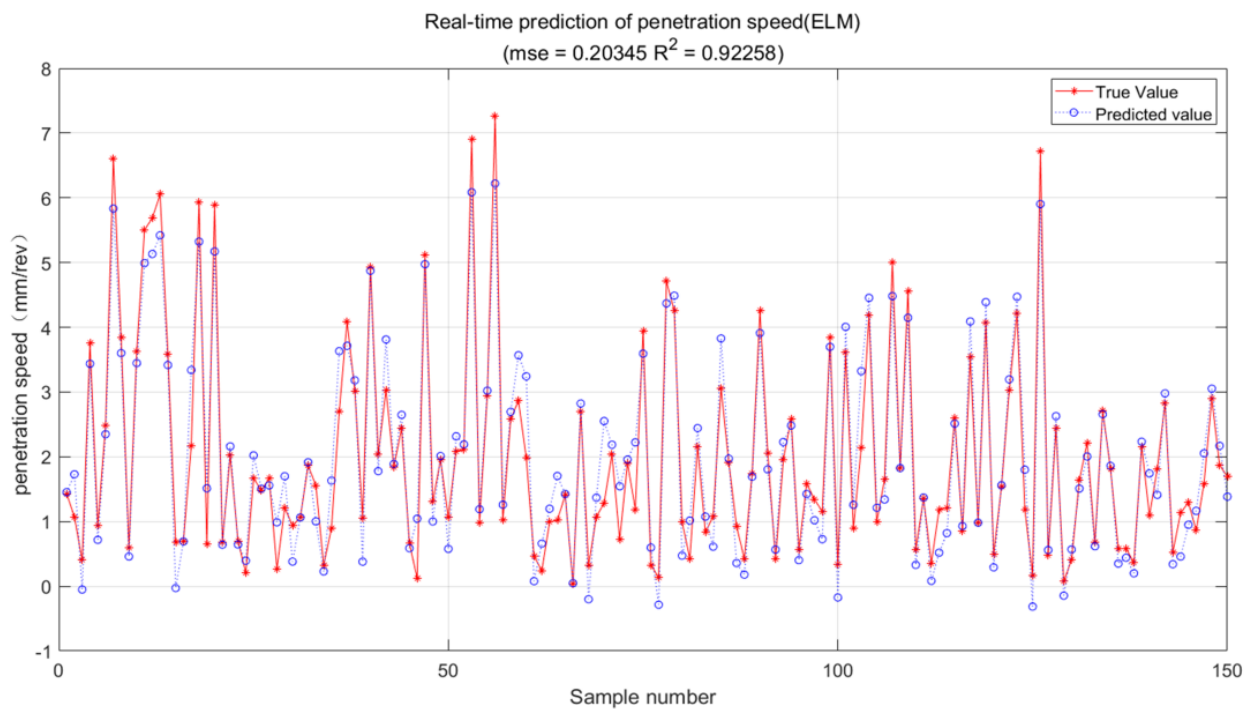


Figure 6. Real-time prediction of the penetration speed.

In the comparison of the real value of the predicted value of the penetration speed, the horizontal coordinate is the sample number of the test set, there are a total of 150 samples, and the vertical coordinate is the predicted value and the real value of the penetration speed of each sample. It can be seen from the figure that the gap between the predicted value and the real value of the penetration speed is small, and the predicted results of the penetration speed can reflect the real penetration speed, to a certain extent. Following the calculation, the *MSE* of the prediction result of 150 groups of data is 0.2, and R^2 is 0.92. the prediction model has a good accuracy.

Similarly, with the same sampling method and the principle, this paper carries on the prediction experiment on the working torque, working pressure and rotational speed of the drilling in the reaming up process.

3.4.2. Prediction of the Working Torque

In the reaming stage of the RBM, the main use of the drill pipe is to transfer the output power of the drill to the bit, by applying a certain rotating torque and driving force to make the bit rotate and break the rock. In addition, the drill pipe mostly adopts a hollow tubular structure, which is responsible for the transmission of the drilling fluid in the guide hole and reaming stage. The working torque refers to the torque input of the reaming bit under the condition of a certain drilling rate. The working torque varies with the rock properties and the rock breaking pressure, and the torque also reflects the energy needed for the bit to break the rock. Therefore, the prediction of the working torque borne by the drill pipe in the drilling process can help the operator to select the appropriate drilling tool system.

When predicting the working torque, the working torque is taken as the output of the ELM algorithm model, and the working pressure, rotational speed of the drilling and the penetration speed are taken as the input of the ELM algorithm model. One thousand eight hundred and fifty groups out of 2000 groups were randomly selected as the training set, and the remaining 150 groups were selected as the test set. The comparison of the real value of the predicted working torque of the test set is shown in the Figure 7.

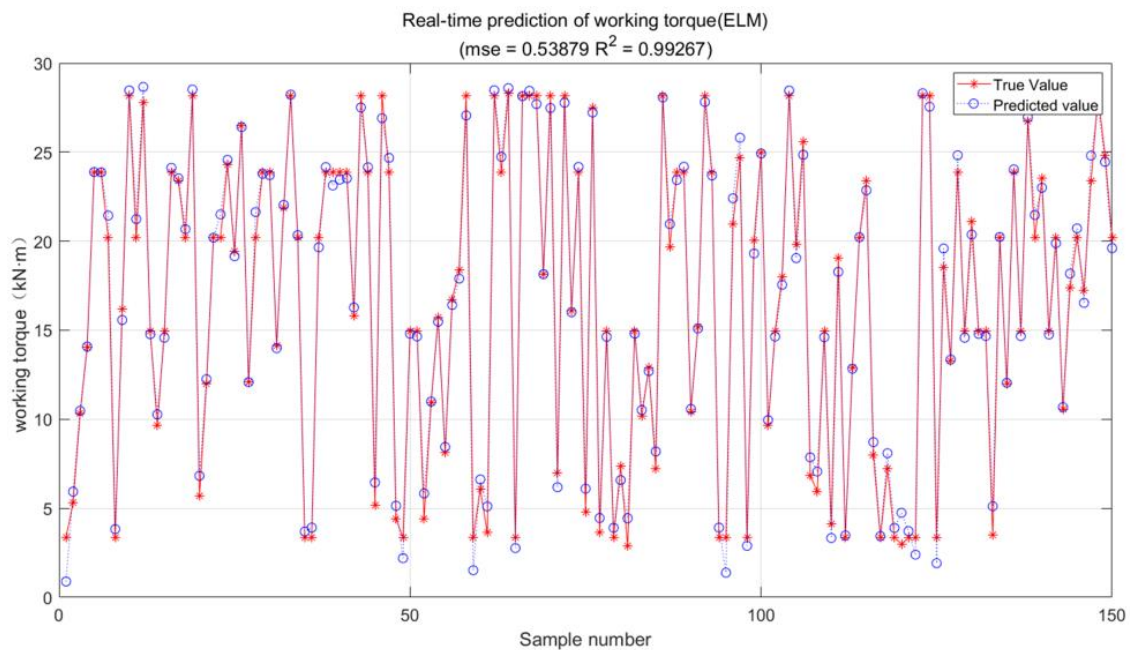


Figure 7. Real-time prediction of the working torque.

From the comparison of the real value of the working torque predicted by the test set, we can see that the gap between the working torque predicted by the ELM algorithm model and the real value is small, and the predicted results of the torque can accurately reflect the real working torque, to a certain extent. Following the calculation, the *MSE* of the prediction results of 150 groups of data is 0.53 and R^2 is 0.99. The prediction model also has a good accuracy.

3.4.3. Prediction of the Working Pressure

The working pressure is the sum of the pressure exerted by the drill bit on the rock surface at the bottom of the shaft. The working pressure is distributed on the rock-breaking hobs of the drill bit device, and the teeth on the hobs are pressed into the rock by the rotation of the drill bit, thus effectively breaking the rock. When predicting the working pressure in the process of ream drilling, the working pressure is taken as the output of the ELM algorithm model, and the working torque, the penetration speed and the rotational speed of the drilling are taken as the input of the ELM algorithm model. Similarly, 1850 groups out of 2000 sets were randomly selected as the training set, and the remaining 150 groups were selected as the test set. The comparison of the real value of the predicted working pressure of the test set is shown in the Figure 8.

From the comparison of the real value of the predicted value of the test set, we can see that the gap between the predicted value and the real value is small, and the predicted results can reflect the real size of the working pressure, to a certain extent. Following the calculation, the *MSE* of the prediction results of 150 groups of data is 19.7, and R^2 is 0.99. In this prediction experiment, because the values of the pulling force of the reaming are large, there is a certain deviation between the predicted value and the actual value, but the ratio of the deviation to the working pressure is still small, considering that R^2 is 0.99, so the prediction model is also accurate.

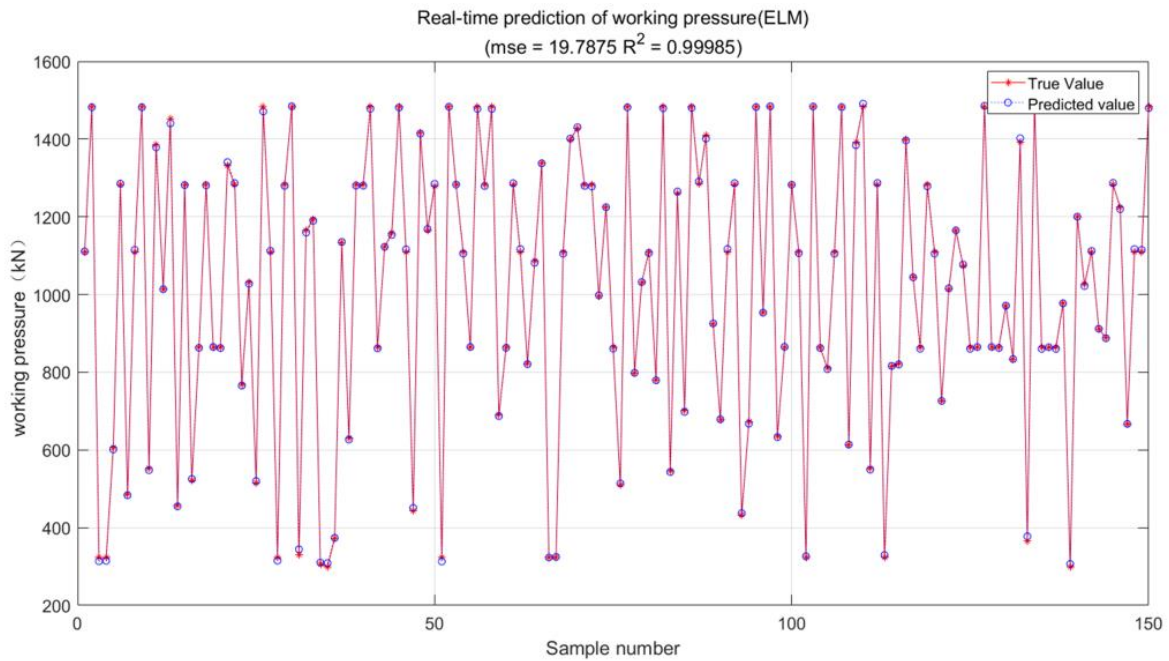


Figure 8. Real-time prediction of the working pressure.

3.4.4. Prediction of the Rotational Speed of Drilling

The output speed of the RBM should meet the needs of the guide hole drilling and the ream drilling. When predicting the rotational speed in the process of ream drilling, the rotational speed of the drilling is taken as the output of the ELM algorithm model, and the working torque, working pressure and penetration speed are taken as the input of the ELM algorithm model. Similarly, 1850 groups out of 2000 sets of data were run were randomly selected as the training set, and the remaining 150 groups were used as the test set. The real value of the predicted rotational speed of the test set is shown in Figure 9:

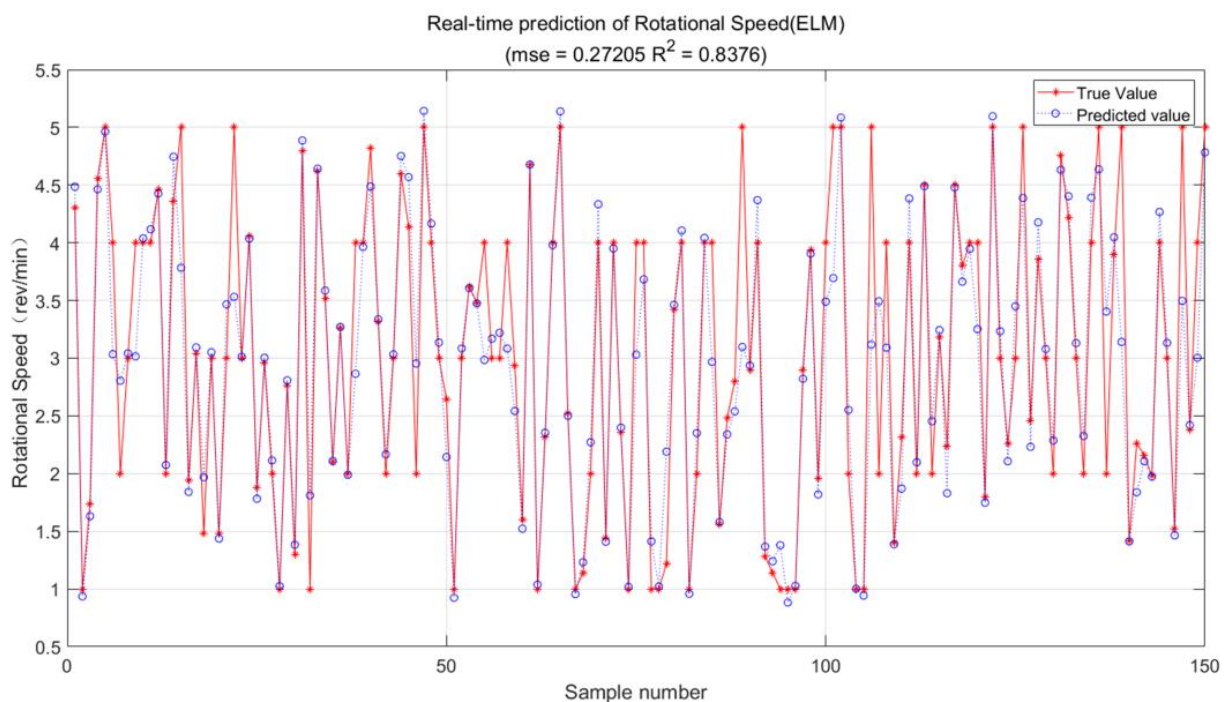


Figure 9. Real-time prediction of the rotational speed.

The experimental results shown above are the results obtained when the number of neurons in the hidden layer is set to 10 in the process of using the ELM algorithm, to predict the rotational speed. It can be seen from the diagram that R^2 is only 0.83 and the prediction result is not accurate. The network structure is re-adjusted and the number of neurons in the hidden layer is set to 50. The final result shows that R^2 is greater than 0.9 to meet the prediction requirements. The comparison of the real predicted value of the optimized rotational speed of the test set is shown in the Figure 10.

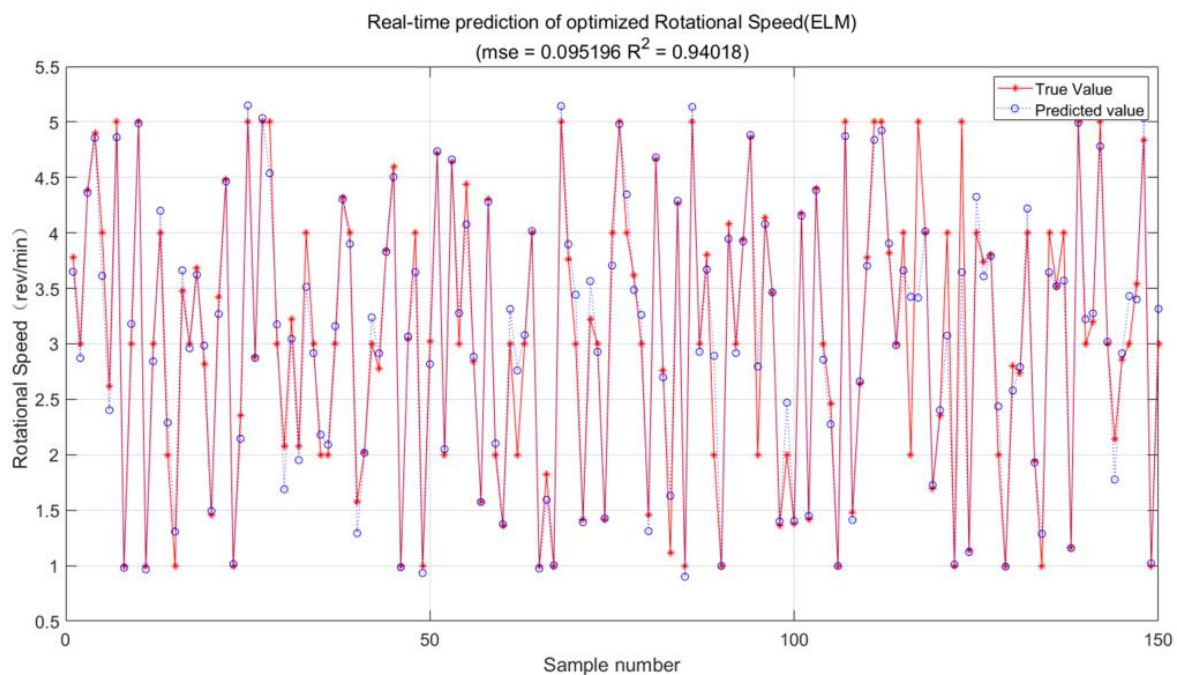


Figure 10. Real-time prediction of the optimized rotational speed.

In the process of using the ELM to predict the drilling parameters of the RBM, the model is trained by the established training set, then the model is tested by the test set, and then the network structure parameters of the ELM are adjusted until the prediction accuracy of the test set meets the experimental requirements. Finally, the input weight matrix IW , bias matrix B and hidden layer weight matrix LW in the ELM model are determined. Finally, the successful prediction model can be used to predict the relevant parameters of the ream drilling.

During the working process of the drilling rig, after the data of the working pressure, working torque, rotational speed of drilling and penetration speed are collected by the sensor, they are predicted by the prediction model of the working parameters of the extreme learning machine established above, the optimized operating parameters of the drilling rig can be obtained. the drilling efficiency of the RBM can be improved, to a certain extent, by using this parameter.

3.5. Intelligent Monitoring of the Bit Status

When the reaming drills are used for drilling in hard rock, bit bouncing often occurs, the drilling rig can overcome the resistance torque of the rock by gradually increasing the torque, and the bit returns to a normal working condition. However, when the increasing torque of the drill pipe is not enough to overcome the resistance moment of the rock, and if the relevant operation is not taken in time, the power of the drill rig may break, even the drill pipe can break. It is of great practical significance to be able to determine whether the bit is faulty or not. By using the classification algorithm model of the ELM and KELM, we analyze and process the simulated sensor data of the drilling rig, and obtain the intelligent monitoring of the drilling rig's working condition.

3.5.1. Monitoring Experiment of the Drilling Status based on the ELM

In this work, the model classification training of the ELM is carried out by using simulation sensor data. A total of 400 sets out of 200 sets of data, from normal and faulty conditions, were used for the experiment. Different from the previous ELM prediction model, the simulation data need to be marked first in the experiment. The working condition of the drilling rig is simplified, which is only divided into normal working conditions and faulty conditions. The working torque, working pressure, penetration speed and rotational speed of the drilling sensor data corresponding to the normal operating conditions are marked as 1, and the relevant sensor data corresponding to the faulty conditions are marked as 2. When the classification algorithm model of the ELM is used to monitor the working conditions of the drilling rig, the input of the model is the sensor data of working pressure, working torque, rotational speed of drilling and penetration speed under the different working conditions, and the output of the model is the corresponding working condition label. The randperm function is used to randomly select 360 groups of data as the training data set, and the remaining 40 groups of data are used as the test set to classify the working conditions of the RBM. The experimental results are shown in the Figure 11.

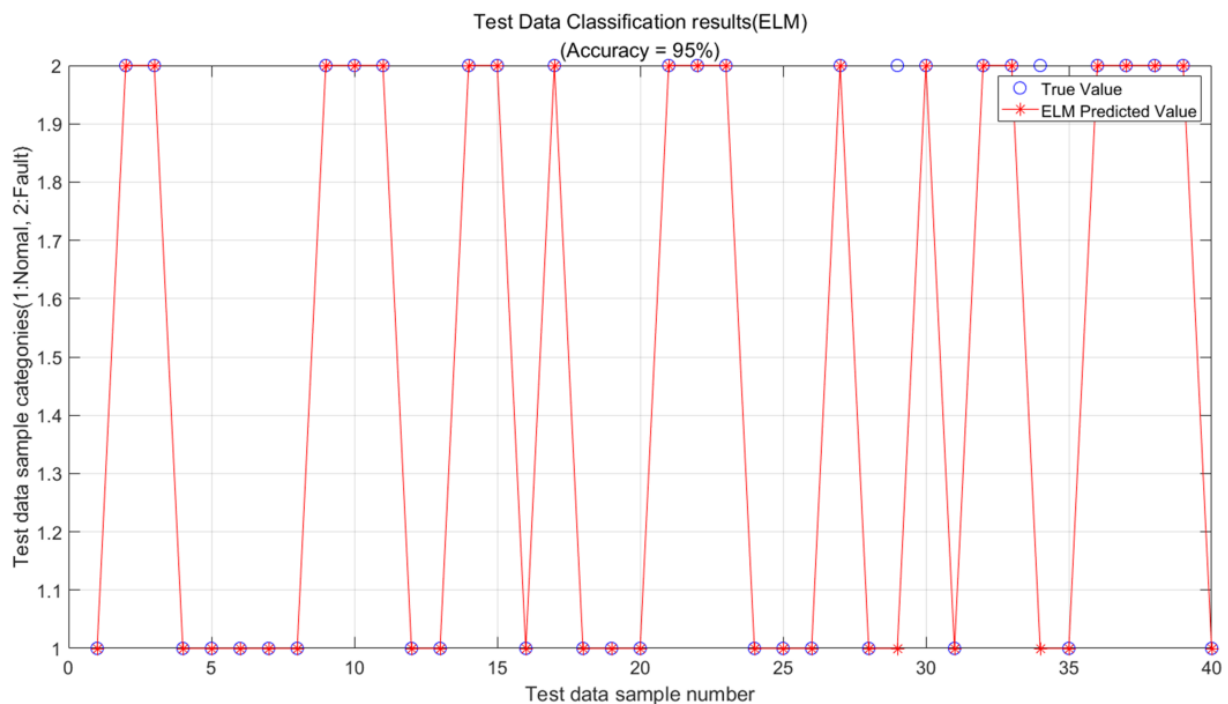


Figure 11. Comparison of the predicted and true values of the test data(ELM).

In the comparison between the real value and the predicted value, the horizontal coordinate is the sample number of the test set, and the vertical coordinate is the bit working condition category corresponding to each sample, where 1 indicates that the bit is in normal working condition and 2 indicates that the bit is in a faulty condition. It can be seen from the figure that among the 40 sets of data in the test set, 38 sets of the ELM algorithm models are predicted correctly, another two groups demonstrate faulty conditions, and the algorithm is predicted to be in a normal condition, and the overall prediction accuracy is 95%. This is because by using the ELM in the model training, each training will randomly specify the connection weight between the input layer and the hidden layer and the threshold of the hidden layer.

3.5.2. Optimal Monitoring Experiment of the Drilling Status based on the KELM

For this reason, we use the KELM to optimize the working condition classification experiment of 400 groups of simulation sensor data. Similarly, the randperm function is used to randomly select 360 groups of data as the training data set, and the remaining 40 groups of data as the test set. The experimental results are shown in the Figure 12.

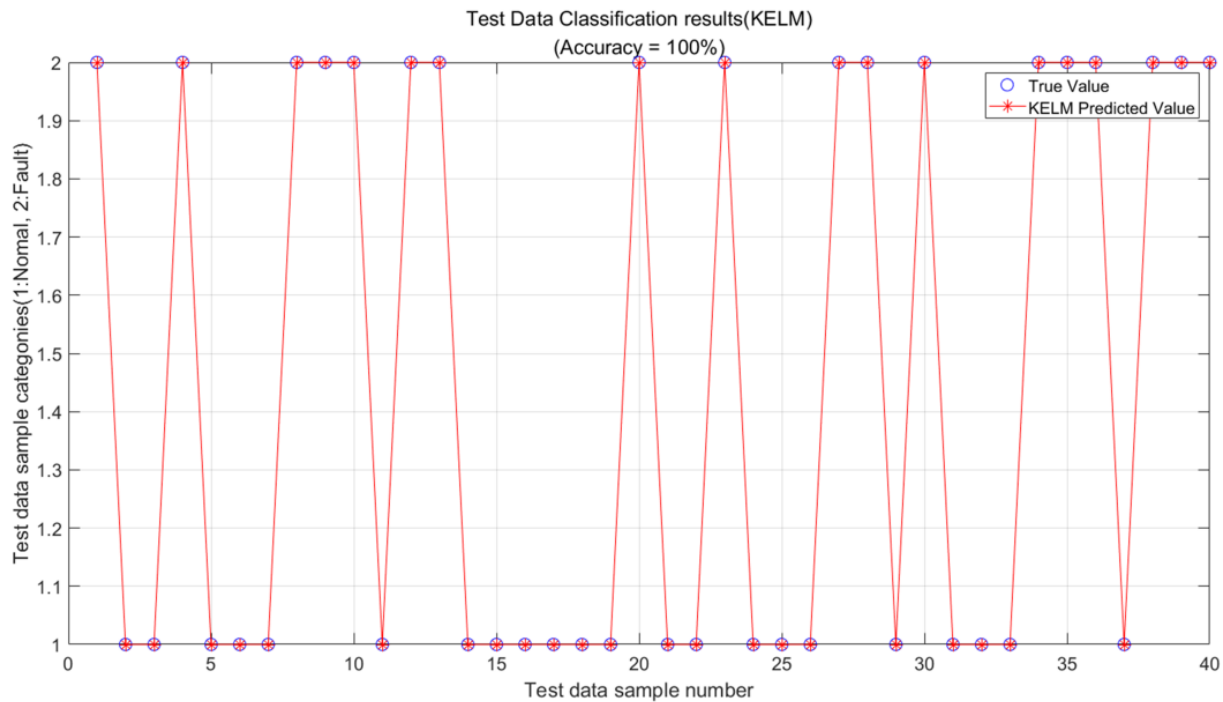


Figure 12. Comparison of the predicted and true values of the test data(KELM).

From the comparison chart of the classification prediction results of the KELM, we can see that the prediction results are completely consistent with the real operating conditions, and the classification accuracy of the model is 100%. From the experimental results, it can be seen that the classification of the bit's working conditions in the drilling process, by using the KELM, is more accurate than the ELM.

4. Discussion

The experimental results show that firstly, a strong learning ability is demonstrated in the regression prediction task of the RBM technical parameters using the ELM. We have compiled the four most important technical parameters for the RBM ream drilling, which are the working pressure, working torque, penetration speed and rotational speed, which have a non-linear relationship with each other. We have also organized the real-time data during the work, also in the process of training using the ELM, with the aim of calculating the weights between the implied layer and the output layer. The prediction phase, moreover, is designed to use the weights between the implicit and the output layers, to calculate the output, i.e., the parameters we need to predict. In the experimental phase, first we predict the value of the drilling speed, based on the data of the rotational speed, the working torque and working pressure, and then we use the MSE and R^2 to make trade-offs so as to determine whether the prediction model meets the requirements. In the prediction experiment for the penetration speed, we can see from the results that the MSE is only 0.2 and R^2 is 0.92, which shows that the prediction model is very successful, according to the trade-off condition. Secondly, we conducted a classification experiment using the ELM, which is divided into a normal condition and a faulty condition. We conducted the experiment using 400 sets of data, and from the experimental results, we can see that the

accuracy of the ELM is only 95%, while the accuracy of the KELM is 100%, and it is better to use the KELM to classify the bit's working condition during the drilling process.

The KELM is more stable and has a better generalization ability when performing predictions for the classification experiments. In the RBM hole expansion drilling process, most of the previous work is based on empirical models, which cannot make accurate predictions of the main technical parameters, and is still in its infancy for intelligent control, hence this paper takes the intelligent algorithm as the starting point to improve the efficiency of the RBM.

5. Conclusions

This research first uses the training set data to fulfill the construction of the ELM training function, then uses the test set data to test the established prediction function model, improves the prediction accuracy by adjusting the ELM network structure model and the related setting parameters, and finally establishes the ELM algorithm prediction model of the working pressure, working torque, rotational speed of drilling and penetration speed in the reaming process of the RBM. The optimized operating parameters of the drilling rig can be obtained through the prediction model, and the drilling efficiency of the RBM can be improved, to a certain extent. In the predictive regression experimental results, the MSE is 0.2 and the R^2 is 0.92, when predicting the penetration speed, the MSE is 0.53 and the R^2 is 0.99, when predicting the working torque, the MSE is 19.7 and the R^2 is 0.99, when predicting the working pressure, and the MSE is 0.09 and the R^2 is 0.94, when predicting the rotational speed, we can see that the overall prediction effect of the ELM algorithm is very feasible.

Furthermore, by calibrating the drilling data and using the ELM classification algorithm model to train the working condition data of the drilling rig, a working condition monitoring model, based on the ELM algorithm is established. On this basis, the working condition monitoring model, based on the KELM algorithm is constructed, and the working condition monitoring model of the ELM algorithm is optimized. By feeding the sensor data in the working process of the drilling rig into the KELM working condition monitoring model, we can judge whether the bit is in a normal or faulty condition. When it is judged that the bit is in a normal working condition, the construction can be continued, according to the predicted construction parameters. When judging that the bit is in a faulty condition, it is necessary to adjust the parameters on the operator console, to make sure that the bit is not in a continuous faulty condition. From the experimental results, the prediction success rate of the KELM is 5% more than that of the ELM, which effectively proves that the KELM has a higher generalization ability and learning ability. This method greatly improves the accuracy of the reaming status prediction, and plays an important role in the real-time working condition monitoring in the process of ream drilling, and can effectively avoid drilling accidents.

The experimental results have shown that the intelligent predictive control algorithms, based on the ELM and KELM can provide the RBM process planning, construction fault prediction, and fault diagnosis, to power the complex process planning work of RBMs, which will break through the domain knowledge fragmentation and information silos of the industry's long-term experience-dependent decision-making model. The intelligent predictive control algorithm is a new type of algorithm that is constantly updated and iterated, and in the future, more efficient predictive control models may emerge to improve the efficiency of the industry.

However, there are still some open issues in this research. Currently, the technical parameters for rock-breaking in the ream drilling process that we choose, are mainly based on empirical models. A large amount of RBM knowledge is fragmented and scattered, which is difficult to be reused effectively. This also means that there is a lack of effective measures to extract, include, manage and calculate the existing knowledge at the moment. Leveraging the knowledge computing method to effectively combine the adaptive dynamic

planning method and the real-time fault predictions in the RBM process, is an important direction for the future research.

Author Contributions: Conceptualization, G.J. and F.H.; methodology, F.H.; software, W.Y. and F.H.; validation, F.H. and W.Y.; formal analysis, W.Y.; investigation, F.H.; resources G.J.; data curation, W.Y.; writing original draft preparation, F.H., G.J. and W.Y.; writing review and editing, F.H., G.J. and W.Y.; visualization, F.H. and G.J.; supervision, F.H. and G.J.; project administration, F.H. and G.J.; funding acquisition, F.H. and G.J. All authors have read and agreed to the published version of the manuscript.

Funding: The project was supported by the National Key Research and Development Program of China (Grant No. 2016YFC0600802) and by the self-supported project for the mine construction division of Tiandi Technology Co., Ltd.(Grant No. KJ-2021-JJZD-02).

Data Availability Statement: All data generated or analyzed during this study are included in this article.

Conflicts of Interest: The authors declare no conflict of interest.

References

- Liu, Z.; Meng, Y. Key technologies of drilling process with raise boring method. *J. Rock Mech. Geotech. Eng.* **2015**, *7*, 385–394. [\[CrossRef\]](#)
- Jing, G.; Hu, F.; Chen, Y. Failure analysis and revamping methods for loading threaded joints of raiseboring machine. In Proceedings of the IOP Conference Series: Earth and Environmental Science, Changchun, China, 21–23 August 2020; IOP Publishing: Bristol, UK, 2020; Volume 546, p. 052064. [\[CrossRef\]](#)
- Jing, G.; Qiu, X.; Hu, F.; Liu, W. Strain measurement and experimental analysis of buttress thread joints of drill rods. In Proceedings of the 2021 3rd International Academic Exchange Conference on Science and Technology Innovation (IAECST), Guangzhou, China, 10–12 December 2021; IEEE: Piscataway, NJ, USA, 2021; pp. 859–867. [\[CrossRef\]](#)
- Hu, X.-K.; Liu, Z.-Q.; Tan, H. Influence of engineering parameters on rock breaking performance of raise boring machine. *Measurement* **2021**, *174*, 109005. [\[CrossRef\]](#)
- Hu, F.; Qiu, X.; Jing, G.; Tang, J.; Zhu, Y. Digital twin-based decision making paradigm of raise boring method. *J. Intell. Manuf.* **2022**, 1–19. [\[CrossRef\]](#)
- Shaterpour-Mamaghani, A.; Bilgin, N.; Balci, C.; Avunduk, E.; Polat, C. Predicting performance of raise boring machines using empirical models. *Rock Mech. Rock Eng.* **2016**, *49*, 3377–3385. [\[CrossRef\]](#)
- Shaterpour-Mamaghani, A.; Copur, H.; Dogan, E.; Erdogan, T. Development of new empirical models for performance estimation of a raise boring machine. *Tunn. Undergr. Space Technol.* **2018**, *82*, 428–441. [\[CrossRef\]](#)
- Shaterpour-Mamaghani, A.; Copur, H. Empirical performance prediction for raise boring machines based on rock properties, pilot hole drilling data and raise inclination. *Rock Mech. Rock Eng.* **2021**, *54*, 1707–1730. [\[CrossRef\]](#)
- Shaterpour-Mamaghani, A.; Copur, H.; Gumus, A.; Tumac, D.; Balci, C.; Erdogan, T.; Dogan, E.; Kocbay, A. Full-Scale linear cutting tests using a button cutter and deterministic performance prediction modeling for raise boring machines. *Tunn. Undergr. Space Technol.* **2022**, *127*, 104609. [\[CrossRef\]](#)
- Mayne, D.Q. Model predictive control: Recent developments and future promise. *Automatica* **2014**, *50*, 2967–2986. [\[CrossRef\]](#)
- Morari, M.; Lee, J.H. Model predictive control: Past, present and future. *Comput. Chem. Eng.* **1999**, *23*, 667–682. [\[CrossRef\]](#)
- Qin, S.J.; Badgwell, T.A. A survey of industrial model predictive control technology. *Control. Eng. Pract.* **2003**, *11*, 733–764. [\[CrossRef\]](#)
- Maxim, A.; Copot, D.; Copot, C.; Ionescu, C.M. The 5w’s for control as part of industry 4.0: Why, what, where, who, and when—A PID and MPC control perspective. *Inventions* **2019**, *4*, 10. [\[CrossRef\]](#)
- Zhao, S.; Cajo, R.; De Keyser, R.; Liu, S.; Ionescu, C.M. Nonlinear predictive control applied to steam/water loop in large scale ships. *IFAC-PapersOnLine* **2019**, *52*, 868–873. [\[CrossRef\]](#)
- Liu, L.; Zhang, Q.; Wei, D.; Li, G.; Wu, H.; Wang, Z.; Guo, B.; Zhang, J. Chaotic Ensemble of Online Recurrent Extreme Learning Machine for Temperature Prediction of Control Moment Gyroscopes. *Sensors* **2020**, *20*, 4786. [\[CrossRef\]](#)
- Ionescu, C.M.; Caruntu, C.F.; Cajo, R.; Ghita, M.; Crevecoeur, G.; Copot, C. Multi-objective predictive control optimization with varying term objectives: A wind farm case study. *Processes* **2019**, *7*, 778. [\[CrossRef\]](#)
- Heidari, A.A.; Akhoondzadeh, M.; Chen, H. A Wavelet PM2. 5 Prediction System Using Optimized Kernel Extreme Learning with Boruta-XGBoost Feature Selection. *Mathematics* **2022**, *10*, 3566. [\[CrossRef\]](#)
- Qiu, J.; Yin, X.; Pan, Y.; Wang, X.; Zhang, M. Prediction of Uniaxial Compressive Strength in Rocks Based on Extreme Learning Machine Improved with Metaheuristic Algorithm. *Mathematics* **2022**, *10*, 3490. [\[CrossRef\]](#)
- Chen, Y.; Zhou, Y.; Zhang, Y. Machine learning-based model predictive control for collaborative production planning problem with unknown information. *Electronics* **2021**, *10*, 1818. [\[CrossRef\]](#)

20. Bououden, S.; Chadli, M.; Karimi, H.R. An ant colony optimization-based fuzzy predictive control approach for nonlinear processes. *Inf. Sci.* **2015**, *299*, 143–158. [[CrossRef](#)]
21. Ejigu, D.A.; Liu, X. Gradient descent-particle swarm optimization based deep neural network predictive control of pressurized water reactor power. *Prog. Nucl. Energy* **2022**, *145*, 104108. [[CrossRef](#)]
22. Zhang, R.; Zou, H.; Xue, A.; Gao, F. GA based predictive functional control for batch processes under actuator faults. *Chemom. Intell. Lab. Syst.* **2014**, *137*, 67–73. [[CrossRef](#)]
23. Feng, K.; Lu, J.; Chen, J. Nonlinear model predictive control based on support vector machine and genetic algorithm. *Chin. J. Chem. Eng.* **2015**, *23*, 2048–2052. [[CrossRef](#)]
24. Lin, Y.; Chen, D.-D.; Chen, M.-S.; Chen, X.-M.; Li, J. A precise BP neural network-based online model predictive control strategy for die forging hydraulic press machine. *Neural Comput. Appl.* **2018**, *29*, 585–596. [[CrossRef](#)]
25. Peng, H.; Wu, J.; Inoussa, G.; Deng, Q.; Nakano, K. Nonlinear system modeling and predictive control using the RBF nets-based quasi-linear ARX model. *Control. Eng. Pract.* **2009**, *17*, 59–66. [[CrossRef](#)]
26. Yang, Y.; Lin, X.; Miao, Z.; Yuan, X.; Wang, Y. Predictive control strategy based on extreme learning machine for path-tracking of autonomous mobile robot. *Intell. Autom. Soft Comput.* **2015**, *21*, 1–19. [[CrossRef](#)]
27. Wong, P.K.; Wong, H.C.; Vong, C.M.; Xie, Z.; Huang, S. Model predictive engine air-ratio control using online sequential extreme learning machine. *Neural Comput. Appl.* **2016**, *27*, 79–92. [[CrossRef](#)]
28. Yan, Z.; Wang, J. Robust model predictive control of nonlinear systems with unmodeled dynamics and bounded uncertainties based on neural networks. *IEEE Trans. Neural Netw. Learn. Syst.* **2013**, *25*, 457–469. [[CrossRef](#)]
29. Chen, M.-R.; Zeng, G.-Q.; Lu, K.-D.; Weng, J. A two-layer nonlinear combination method for short-term wind speed prediction based on ELM, ENN, and LSTM. *IEEE Internet Things J.* **2019**, *6*, 6997–7010. [[CrossRef](#)]
30. Tian, H.-X.; Mao, Z.-Z. An ensemble ELM based on modified AdaBoost. RT algorithm for predicting the temperature of molten steel in ladle furnace. *IEEE Trans. Autom. Sci. Eng.* **2009**, *7*, 73–80. [[CrossRef](#)]
31. Djerioui, M.; Bouamar, M.; Ladjal, M.; Zerguine, A. Chlorine soft sensor based on extreme learning machine for water quality monitoring. *Arab. J. Sci. Eng.* **2019**, *44*, 2033–2044. [[CrossRef](#)]
32. Gao, Z.; Hu, Q.; Xu, X. Condition monitoring and life prediction of the turning tool based on extreme learning machine and transfer learning. *Neural Comput. Appl.* **2022**, *34*, 3399–3410. [[CrossRef](#)]
33. Montazeri-Gh, M.; Nekoonam, A. Gas path component fault diagnosis of an industrial gas turbine under different load condition using online sequential extreme learning machine. *Eng. Fail. Anal.* **2022**, *135*, 106115. [[CrossRef](#)]
34. Cao, J.; Lin, Z.; Huang, G.-B.; Liu, N. Voting based extreme learning machine. *Inf. Sci.* **2012**, *185*, 66–77. [[CrossRef](#)]
35. Huang, G.-B.; Zhu, Q.-Y.; Siew, C.-K. Extreme learning machine: A new learning scheme of feedforward neural networks. In Proceedings of the 2004 IEEE International Joint Conference on Neural Networks (IEEE Cat. No. 04CH37541), Budapest, Hungary, 25–29 July 2004; IEEE: Piscataway, NJ, USA, 2004; Volume 2, pp. 985–990. [[CrossRef](#)]
36. Huang, G.; Huang, G.-B.; Song, S.; You, K. Trends in extreme learning machines: A review. *Neural Netw.* **2015**, *61*, 32–48. [[CrossRef](#)]
37. Huang, G.-B.; Zhu, Q.-Y.; Siew, C.-K. Extreme learning machine: Theory and applications. *Neurocomputing* **2006**, *70*, 489–501. [[CrossRef](#)]
38. Zhu, Q.-Y.; Qin, A.K.; Suganthan, P.N.; Huang, G.-B. Evolutionary extreme learning machine. *Pattern Recognit.* **2005**, *38*, 1759–1763. [[CrossRef](#)]
39. Zhang, S.; Sun, T.; Li, Y.; Sui, X. Adaptive Voting Online Sequential Extreme Learning Machine based on Glowworm Swarm Optimization Selective Ensemble Algorithm. In Proceedings of the 2020 IEEE International Conference on Systems, Man, and Cybernetics (SMC), Toronto, ON, Canada, 11–14 October 2020; IEEE: Piscataway, NJ, USA, 2020; pp. 1473–1478. [[CrossRef](#)]
40. Li, J.; Cheng, J.-H.; Shi, J.-Y.; Huang, F. Brief introduction of back propagation (BP) neural network algorithm and its improvement. In *Advances in Computer Science and Information Engineering*; Springer: Berlin/Heidelberg, Germany, 2012; pp. 553–558. [[CrossRef](#)]
41. Ding, S.; Su, C.; Yu, J. An optimizing BP neural network algorithm based on genetic algorithm. *Artif. Intell. Rev.* **2011**, *36*, 153–162. [[CrossRef](#)]
42. Huang, G.-B. An insight into extreme learning machines: Random neurons, random features and kernels. *Cogn. Comput.* **2014**, *6*, 376–390. [[CrossRef](#)]
43. Kongsorot, Y.; Horata, P.; Musikawan, P.; Sunat, K. Kernel extreme learning machine based on fuzzy set theory for multi-label classification. *Int. J. Mach. Learn. Cybern.* **2019**, *10*, 979–989. [[CrossRef](#)]
44. Kang, F.; Liu, X.; Li, J. Temperature effect modeling in structural health monitoring of concrete dams using kernel extreme learning machines. *Struct. Health Monit.* **2020**, *19*, 987–1002. [[CrossRef](#)]
45. Fu, H.; Vong, C.-M.; Wong, P.-K.; Yang, Z. Fast detection of impact location using kernel extreme learning machine. *Neural Comput. Appl.* **2016**, *27*, 121–130. [[CrossRef](#)]
46. Shamshirband, S.; Mohammadi, K.; Chen, H.-L.; Samy, G.N.; Petković, D.; Ma, C. Daily global solar radiation prediction from air temperatures using kernel extreme learning machine: A case study for Iran. *J. Atmos. Sol.-Terr. Phys.* **2015**, *134*, 109–117. [[CrossRef](#)]
47. Liu, A.; Zhao, D.; Li, T. A data classification method based on particle swarm optimisation and kernel function extreme learning machine. *Enterp. Inf. Syst.* **2021**, 1–16. [[CrossRef](#)]

48. Zhang, Y.; Wang, Y.; Zhou, G.; Jin, J.; Wang, B.; Wang, X.; Cichocki, A. Multi-kernel extreme learning machine for EEG classification in brain-computer interfaces. *Expert Syst. Appl.* **2018**, *96*, 302–310. [[CrossRef](#)]
49. Chen, H.-L.; Wang, G.; Ma, C.; Cai, Z.-N.; Liu, W.-B.; Wang, S.-J. An efficient hybrid kernel extreme learning machine approach for early diagnosis of Parkinson's disease. *Neurocomputing* **2016**, *184*, 131–144. [[CrossRef](#)]
50. Si, J.; Li, Y.; Ma, S. Intelligent fault diagnosis for industrial big data. *J. Signal Process. Syst.* **2018**, *90*, 1221–1233. [[CrossRef](#)]

Disclaimer/Publisher's Note: The statements, opinions and data contained in all publications are solely those of the individual author(s) and contributor(s) and not of MDPI and/or the editor(s). MDPI and/or the editor(s) disclaim responsibility for any injury to people or property resulting from any ideas, methods, instructions or products referred to in the content.